Quantum metrology with two-mode squeezed thermal state: Parity detection and phase sensitivity*

Heng-Mei Li(李恒梅)[1,†], Xue-Xiang Xu(徐学翔)[2], Hong-Chun Yuan(袁洪春)[3,4], and Zhen Wang(王震)[1]

[1] College of Mathematical Physics and Chemical Engineering, Changzhou Institute of Technology, Changzhou 213002, China
[2] College of Physics and Communication Electronics, Jiangxi Normal University, Nanchang 330022, China
[3] College of Electrical and Optoelectronic Engineering, Changzhou Institute of Technology, Changzhou 213002, China
[4] Changzhou Institute of Modern Optoelectronic Technology, Changzhou 213002, China

(Received 20 March 2016; revised manuscript received 12 May 2016; published online 25 August 2016)

Based on the Wigner-function method, we investigate the parity detection and phase sensitivity in a Mach–Zehnder interferometer (MZI) with two-mode squeezed thermal state (TMSTS). Using the classical transformation relation of the MZI, we derive the input–output Wigner functions and then obtain the explicit expressions of parity and phase sensitivity. The results from the numerical calculation show that supersensitivity can be reached only if the input TMSTS have a large number photons.

Keywords: Mach–Zenhder interferometer, two-mode squeezed thermal state, Wigner function, phase sensitivity

PACS: 42.50.St, 42.50.Dv, 42.50.Lc **DOI:** 10.1088/1674-1056/25/10/104203

1. Introduction

Optical metrology relies on light interferometry as its primary tool for phase estimation.[1,2] A general protocol to estimate an unknown parameter ϕ corresponding to a quantum process in quantum metrology is comprised of three steps.[3,4] Firstly, a quantum state ρ, which plays an important role in the measurement scheme, is prepared that will serve as the probe. Secondly, this probe state interacts with a system of interest such that ρ evolves to a state ρ_ϕ which depends on the parameter ϕ to be estimated. In the third and last step, an observable O of the probe state is measured in order to gain information about the value of ϕ. Therefore, the phase sensitivity $\delta\phi$ of an interferometer, followed by a detection scheme described by an operator O, can be characterized using the error propagation formula[5]

$$\delta\phi^2 = \frac{\langle O^2\rangle - \langle O\rangle^2}{\left(\partial_\phi \langle O\rangle\right)^2}, \tag{1}$$

which is the ratio of the signal noise to how the signal changes with respect to ϕ. In general, one benchmark for the phase sensitivity is the shot-noise limit (SNL), namely $\delta\phi_{\rm SNL} = 1/\sqrt{\bar{N}}$, where $\bar{N}$ is the average number of photons. Another benchmark for the phase sensitivity is the Heisenberg limit (HL), namely $\delta\phi_{\rm HL} = 1/\bar{N}$.[6] In reference of these two benchmarks, one main aim of the phase sensitivity is to study the relationship between $\delta\phi$ and $\bar{N}$.

The usual tool to estimate phase is the physical process of quantum interference by using a Mach–Zenhder interferometer (MZI).[7] Enormous efforts have been devoted to improve the sensitivity of the interferometers by using a different input light field. In 1981, Caves pointed out that by using coherent light together with a squeezed vacuum one could beat SNL $\delta\phi < \delta\phi_{\rm SNL}$ (supersensitivity).[8] Similar works had been also studied by Pezzé *et al.*[9] and Seshadreesan *et al.*,[10] which showed that the phase sensitivity can reach the Heisenberg limit. In the work of Boto *et al.*,[11] it is possible to beat SNL by exploiting special states of light, such as the $N00N$ state.[12] Hu *et al.* investigated quantum interference with Fock and conventional cat states,[13] where the phase sensitivity approaches to the HL with the increasing values of Fock number and the total average photon number, and Lee *et al.* demonstrated the more enhanced performance in phase estimation by using a four-headed cat state rather than the conventional cat state.[14] In addition, some works show that entanglement is important in order to achieve supersensitivity.[15]

Recently, both Anisimov *et al.*[16] and Zhang *et al.*[17] studied the sensitivity of phase measurement in an MZI with a two-mode squeezed vacuum state (TMSVS). The former scheme showed that sub-Heisenberg sensitivity was obtained with parity detection, the latter one presented that phase sensitivity was obtained with the $\widehat{S}_z^2$ measurement, which may be useful to estimate a small phase shift at high precision. As an extension of that work, we shall study the similar work with a two-mode squeezed thermal state (TMSTS) as the input resource. Therefore, the TMSVS is only a special case of our present work. It is emphasized that we shall tackle such input–output issues by using the Wigner-function (WF) method,[18] which can be viewed as a quantum analogy to the operational

*Project supported by the National Natural Science Foundation of China (Grant No. 11447002), the Research Foundation of the Education Department of Jiangxi Province of China (Grant No. GJJ150338), and the Research Foundation for Changzhou Institute of Modern Optoelectronic Technology (Grant No. CZGY15).

†Corresponding author. E-mail: lihengm@ustc.edu.cn

© 2016 Chinese Physical Society and IOP Publishing Ltd

formulation of classical mechanics.[19,20] Very recently, our group carried out some similar works on the phase estimation with the phase space method.[21,22]

In this paper, we shall focus on demonstrating the utility of the WF method in studying the parity detection and the phase sensitivity of MZI with TMSTS as the input resource. The paper is organized as follows. In Section 2 we make a brief review of the two-mode squeezed thermal state (TMSTS) and derive its WF after obtaining its normal ordering form. In Section 3, we simply obtain the output WF after employing the input–output transformation. In Section 4, the analytical expression of the parity is obtained. Then the analytical expression of the phase sensitivity is obtained in Section 5. Finally, our results are summarized in Section 6.

2. Two-mode squeezed thermal state

In this section, we give a brief description of the two-mode squeezed thermal states and derive its normal ordering form and Wigner function.

2.1. Description of TMSTS

The density operator of the TMSTS[23,24] is given by

$$\rho = S(r)\,\rho_{\mathrm{th}1}\rho_{\mathrm{th}2}S^{\dagger}(r), \tag{2}$$

where $S(r)=\exp\left[r\left(a^{\dagger}b^{\dagger}-ab\right)\right]$ is the two-mode squeezed operator with real squeezing parameter r, whose transformation relations are

$$\begin{aligned} S(r)\,a^{\dagger}S^{\dagger}(r) &= a^{\dagger}\cosh r - b\sinh r,\\ S(r)\,b^{\dagger}S^{\dagger}(r) &= b^{\dagger}\cosh r - a\sinh r. \end{aligned} \tag{3}$$

Here $\rho_{\mathrm{th}\,j}$ $(j=1,2)$ is a density operator of single-mode thermal state,

$$\rho_{\mathrm{th}\,j} = \sum_{n=0}^{\infty}\frac{\bar{n}_j^n}{(\bar{n}_j+1)^{n+1}}\left|n\right\rangle\left\langle n\right|, \tag{4}$$

where $\bar{n}_j$ is the average photon number of the thermal state $\rho_{\mathrm{th}\,j}$. When $\bar{n}_1=\bar{n}_2=0$, $\rho_{\mathrm{th}1}\rho_{\mathrm{th}2}\to\left|0,0\right\rangle\left\langle 0,0\right|$, TMSTS reduces to TMSVS. If the average photon number of $\rho_{\mathrm{th}\,j}$ is identical $\bar{n}_1=\bar{n}_2=\bar{n}$, then TMSTS is symmetrical. While $\bar{n}_1\neq\bar{n}_2$, then TMSTS is asymmetrical.

In addition, the P-representation of density operator $\rho_{\mathrm{th}\,j}$ can be expanded as

$$\rho_{\mathrm{th}\,j} = \frac{1}{\bar{n}_j}\int\frac{\mathrm{d}^2\alpha_j}{\pi}\exp\left(-\frac{1}{\bar{n}}\left|\alpha_j\right|^2\right)\left|\alpha_j\right\rangle\left\langle\alpha_j\right|, \tag{5}$$

which is useful for later calculation and $\left|\alpha_j\right\rangle$ $(j=1,2)$ are the coherent states. Therefore, $\rho_{\mathrm{th}1}\rho_{\mathrm{th}2}$ can be re-written as

$$\rho_{\mathrm{th}1}\rho_{\mathrm{th}2} = \int\frac{\mathrm{d}^2\alpha_1\,\mathrm{d}^2\alpha_2}{\pi^2}P(\alpha_1,\alpha_2)\left|\alpha_1,\alpha_2\right\rangle\left\langle\alpha_1,\alpha_2\right| \tag{6}$$

with the P-representation of two-mode thermal state (TMTS)

$$P(\alpha_1,\alpha_2) = \exp(-\left|\alpha_1\right|^2/\bar{n}_1-\left|\alpha_2\right|^2/\bar{n}_2)/(\bar{n}_1\bar{n}_2)$$

and $\left|\alpha_1,\alpha_2\right\rangle=\left|\alpha_1\right\rangle\otimes\left|\alpha_2\right\rangle$. Then we have

$$\rho = \int\frac{\mathrm{d}^2\alpha_1\,\mathrm{d}^2\alpha_2}{\pi^2}P(\alpha_1,\alpha_2)\,S(r)\left|\alpha_1,\alpha_2\right\rangle\left\langle\alpha_1,\alpha_2\right|S^{\dagger}(r). \tag{7}$$

Using Eqs. (3) and (7), we can easily obtain the average number of photons for each mode as follows:

$$\begin{aligned} \left\langle a^{\dagger}a\right\rangle &= \bar{n}_1\cosh^2 r+(\bar{n}_2+1)\sinh^2 r,\\ \left\langle b^{\dagger}b\right\rangle &= \bar{n}_2\cosh^2 r+(\bar{n}_1+1)\sinh^2 r, \end{aligned} \tag{8}$$

which leads to the total average photon number for TMSTS

$$\bar{N} = (\bar{n}_1+\bar{n}_2)\cosh 2r+2\sinh^2 r. \tag{9}$$

In particular when $\bar{n}_1=\bar{n}_2=0$, it reduces to the TMSVS with average photon number $2\sinh^2 r$.

2.2. Normal ordering form of TMSTS

In order to simplify our calculation, here we shall derive the normally ordering form of TMSTS. Noting that the integration of squeezing operator[25]

$$S(r) = \int\frac{\mathrm{d}^2\eta}{\pi\,\mathrm{e}^r}\left|\frac{\eta}{\mathrm{e}^r}\right\rangle\left\langle\eta\right| \tag{10}$$

with

$$\left|\eta\right\rangle = \exp\left(-\frac{\left|\eta\right|^2}{2}+\eta a^{\dagger}-\eta^{*}b^{\dagger}+a^{\dagger}b^{\dagger}\right)\left|0,0\right\rangle,$$

thus $S(r)\left|\alpha_1,\alpha_2\right\rangle$ can be put into the following form

$$S(r)\left|\alpha_1,\alpha_2\right\rangle = \cosh^{-1}r\exp\left[-\frac{1}{2}\left(\left|\alpha_1\right|^2+\left|\alpha_2\right|^2\right)-\alpha_1\alpha_2\tanh r\right]\exp\left[\left(\alpha_1 a^{\dagger}+\alpha_2 b^{\dagger}\right)\cosh^{-1}r+a^{\dagger}b^{\dagger}\tanh r\right]\left|0,0\right\rangle, \tag{11}$$

where we have used the following integral formula

$$\int\frac{\mathrm{d}^2 z}{\pi}\,\mathrm{e}^{\zeta\left|z\right|^2+\xi z+\eta z^{*}} = -\frac{1}{\zeta}\,\mathrm{e}^{-\xi\eta/\zeta} \tag{12}$$

with $\mathrm{Re}(\zeta)<0$. Thus inserting Eq. (11) and its conjugation into Eq. (7) and using the vacuum projector $\left|0,0\right\rangle\left\langle 0,0\right|=:\exp\left(-a^{\dagger}a-b^{\dagger}b\right):$, where $:\ :$ denotes the normal ordering, as well as the integration with an ordered product of operators (IWOP) technique,[26,27] we obtain

$$\rho = A:\ \exp\left(B_1 a^{\dagger}a+B_2 b^{\dagger}b+B_3 a^{\dagger}b^{\dagger}+B_3 ab\right):, \tag{13}$$

where we have set

$$\begin{aligned} A &= \frac{1}{(\bar{n}_1+\bar{n}_2+1)\cosh^2 r+\bar{n}_1\bar{n}_2},\\ B_1 &= -\frac{(\bar{n}_2-\bar{n}_1+1)+(1+\bar{n}_1+\bar{n}_2)\cosh 2r}{2\,(\bar{n}_1+\bar{n}_2+1)\cosh^2 r+2\bar{n}_1\bar{n}_2}, \end{aligned}$$

$$B_2 = -\frac{(\bar{n}_1-\bar{n}_2+1)+(1+\bar{n}_1+\bar{n}_2)\cosh 2r}{2(\bar{n}_1+\bar{n}_2+1)\cosh^2 r+2\bar{n}_1\bar{n}_2},$$
$$B_3 = \frac{(\bar{n}_1+\bar{n}_2+1)\sinh 2r}{2(\bar{n}_1+\bar{n}_2+1)\cosh^2 r+2\bar{n}_1\bar{n}_2}. \quad (14)$$

The normal ordering form of TMSTS in Eq. (13) can be used to realize our calculations below.

2.3. Wigner function of TMSTS

Knowing the normal ordering form of the density operator, we can easily calculate the Wigner function of the two-mode squeezed thermal state. For a two-mode quantum state ρ, the Wigner function in the coherent state representation is given by the following equation[28]

$$W(\alpha,\beta) = \frac{4\,\mathrm{e}^{2|\alpha|^2+2|\beta|^2}}{\pi^2}\int\frac{\mathrm{d}^2 z_1\,\mathrm{d}^2 z_2}{\pi^2}\,\langle -z_1,-z_2|\,\rho\,|z_1,z_2\rangle\,\mathrm{e}^{-2\left(z_1\alpha^*-z_1^*\alpha\right)-2\left(z_2\beta^*-z_2^*\beta\right)}, \quad (15)$$

where $|z_1,z_2\rangle = |z_1\rangle_a|z_2\rangle_b$ is the two-mode coherent state and $\alpha = (q_1+\mathrm{i}p_1)/\sqrt{2}$, $\beta = (q_2+\mathrm{i}p_2)/\sqrt{2}$. Substituting Eq. (13) into Eq. (15), we obtain the WF of TMSTS as follows:

$$W(\alpha;\beta) = \frac{4H}{\pi^2}\,\mathrm{e}^{J_1|\alpha|^2+J_2|\beta|^2+J_3(\alpha\beta+\alpha^*\beta^*)}, \quad (16)$$

where we have set

$$H = \frac{A}{(2+B_1)(2+B_2)-B_3^2},$$
$$J_1 = \frac{2B_1(2+B_2)-2B_3^2}{(2+B_1)(2+B_2)-B_3^2},$$
$$J_2 = \frac{2B_2(2+B_1)-2B_3^2}{(2+B_1)(2+B_2)-B_3^2},$$
$$J_3 = \frac{4B_3}{(2+B_1)(2+B_2)-B_3^2}. \quad (17)$$

The Gaussian–Wigner function in Eq. (16) shows that TMSTS is a two-mode Gaussian state.

3. Output Wigner function of MZI with the input TMSTS

In this section, based on the phase space method, we derive the output WF of MZI with the TMSTS as an input resource.

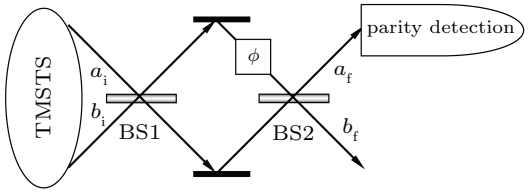


Fig. 1. A lossless Mach–Zehner interferometer with TMSTS as inputs. The modes are labeled by the annihilation operators a_i, b_i for the input port and a_f, b_f for the final output ports, respectively. BS_1 and BS_2 are 50:50 beam splitters. At the output of the MZI, a parity measurement on mode a_f is implemented.

An MZI is composed of optical elements such as beam splitters, mirrors, and phase shifts. As shown in Fig. 1, two input optical modes merge at a 50/50 beam splitter, propagate along two paths of different lengths to accumulate an unknown relative phase shift ϕ, and then merge at a second 50/50 beam splitter. Thus an MZI can be considered as a losses and passive four-port device. Propagating through MZI, two input optical fields (a_i, b_i mode) evolute into two output fields (a_f, b_f mode) yielding

$$\begin{pmatrix} a_f \\ b_f \end{pmatrix} = M_{\mathrm{MZI}}\begin{pmatrix} a_i \\ b_i \end{pmatrix}, \quad (18)$$

where $M_{\mathrm{MZI}} = U_{\mathrm{BS}2}U_\phi U_{\mathrm{BS}1}$ is a unitary scattering matrix composed of several unitary scattering matrices as follows:

$$U_{\mathrm{BS}\,j} = \frac{1}{\sqrt{2}}\begin{pmatrix} 1 & \mathrm{i} \\ \mathrm{i} & 1 \end{pmatrix}, \quad U_\phi = \begin{pmatrix} 1 & 0 \\ 0 & \mathrm{e}^{\mathrm{i}\phi} \end{pmatrix}. \quad (19)$$

The classical correspondence ($a\to\alpha, b\to\beta$) of quantum transformation in Eq. (18) is written as

$$\begin{pmatrix} \alpha_i \\ \beta_i \end{pmatrix} = M_{\mathrm{MZI}}^{-1}\begin{pmatrix} \alpha_f \\ \beta_f \end{pmatrix}, \quad (20)$$

where α_i, β_i, α_f, and β_f represent the complex amplitudes of the field in the modes a_i, b_i, a_f, and b_f, respectively. Therefore, the corresponding transformations of the input–output variables for MZI are given by

$$\alpha_i = -\mathrm{i}\,\mathrm{e}^{-\mathrm{i}\phi/2}\left(-\alpha_f\sin\frac{\phi}{2}+\beta_f\cos\frac{\phi}{2}\right),$$
$$\beta_i = -\mathrm{i}\,\mathrm{e}^{-\mathrm{i}\phi/2}\left(\alpha_f\cos\frac{\phi}{2}+\beta_f\sin\frac{\phi}{2}\right). \quad (21)$$

Propagation of the light field through the optical devices is described by relating the initial variables in the WF to their final expressions,

$$W_{\mathrm{out}}(\alpha_f;\beta_f) = W_{\mathrm{in}}(\alpha_i(\alpha_f;\beta_f);\beta_i(\alpha_f;\beta_f)). \quad (22)$$

Considering the TMSTS as the input resource, the output WF can be obtained by using Eqs. (16) and (21) as well as Eq. (22). Therefore, the state of light at the output of the MZI is described by the following output WF

$$W_{\mathrm{out}}(\alpha_f;\beta_f) = \frac{4H}{\pi^2}\exp\left[\left(J_1\sin^2\frac{\phi}{2}+J_2\cos^2\frac{\phi}{2}\right)|\alpha_f|^2+\frac{J_3\sin\phi}{2}\left(\exp(-\mathrm{i}\phi)\alpha_f^2+\exp(\mathrm{i}\phi)\alpha_f^{*2}\right)\right]$$
$$\times\exp\left[\left(J_1\cos^2\frac{\phi}{2}+J_2\sin^2\frac{\phi}{2}\right)|\beta_f|^2-\frac{J_3\sin\phi}{2}\left(\exp(-\mathrm{i}\phi)\beta_f^2+\exp(\mathrm{i}\phi)\beta_f^{*2}\right)\right]$$

$$\times \exp\left[(J_2 - J_1)\frac{\sin\phi}{2}(\alpha_{\rm f}\beta_{\rm f}^* + \alpha_{\rm f}^*\beta_{\rm f}) - \cos\phi J_3\,(\exp(-{\rm i}\phi)\alpha_{\rm f}\beta_{\rm f} + \exp({\rm i}\phi)\alpha_{\rm f}^*\beta_{\rm f}^*)\right], \tag{23}$$

which also has the Gaussian character. It is obvious to see that the output WF depends on the parameters of the input TMSTS and the shift phase ϕ in this device.

4. Parity detection in one output port

Parity detection should be a better alternative to the detection scheme since parity measurement can determine the evenness or oddness of the photon number in a given beam. Photon number states are assigned a parity of $+1$ if their photon number is even and a parity of -1 if odd. In experiment, using photon-number-resolving detectors or using optical nonlinearities without any photon counting, the parity measurement can be obtained in the low photon number regime. Parity detection was adopted for optical interferometry by Gerry's group.[29]

Here we consider a detector that is placed at one of the output beams in the $a_{\rm f}$ mode. The parity operator for this mode is

$$\Pi_{a_{\rm f}} = (-1)^{a_{\rm f}^\dagger a_{\rm f}} = \exp\left({\rm i}\pi a_{\rm f}^\dagger a_{\rm f}\right), \tag{24}$$

where $a_{\rm f}^\dagger a_{\rm f}$ is the photon number operator for the $a_{\rm f}$ mode. The expected signal of the parity detection scheme can be calculated as the value of the WF for the corresponding mode at the origin. Therefore, the expectation value of the parity operator for the $a_{\rm f}$ mode may be calculated as

$$\langle \Pi_{a_{\rm f}} \rangle = \frac{\pi}{2}\int W_{\rm out}(0;\beta_{\rm f})\,{\rm d}^2\beta_{\rm f}. \tag{25}$$

Performing this operation in calculating the WF in Eq. (23), we obtain the parity for the $a_{\rm f}$ arm

$$\langle \Pi_{a_{\rm f}} \rangle = \frac{2H}{\sqrt{\left(J_1\cos^2\dfrac{\phi}{2} + J_2\sin^2\dfrac{\phi}{2}\right)^2 - J_3^2\sin^2\phi}}. \tag{26}$$

Equation (26) will be used to study the sensitivity of our proposed scheme. In particular, when $\bar{n}_1 = \bar{n}_2 = \bar{n}$, i.e., the symmetrical TMSTS, leading to $J_2 = J_1 = J$, we have

$$\langle \Pi_{a_{\rm f}} \rangle|_{\bar{n}_1=\bar{n}_2=\bar{n}} = \frac{2H}{\sqrt{J^2 - J_3^2\sin^2\phi}}. \tag{27}$$

Let us compare the signal outcomes of the TMSTS with different parameters $(\bar{n}_1, \bar{n}_2, r)$. Specially, when $\bar{n}_1 = \bar{n}_2 = 0$, and $r = 0$, TMSTS is just TMSVS and $\langle \Pi_{a_{\rm f}} \rangle|_{\bar{n}_1=\bar{n}_2=r=0} = 1$, i.e., it always remains one.

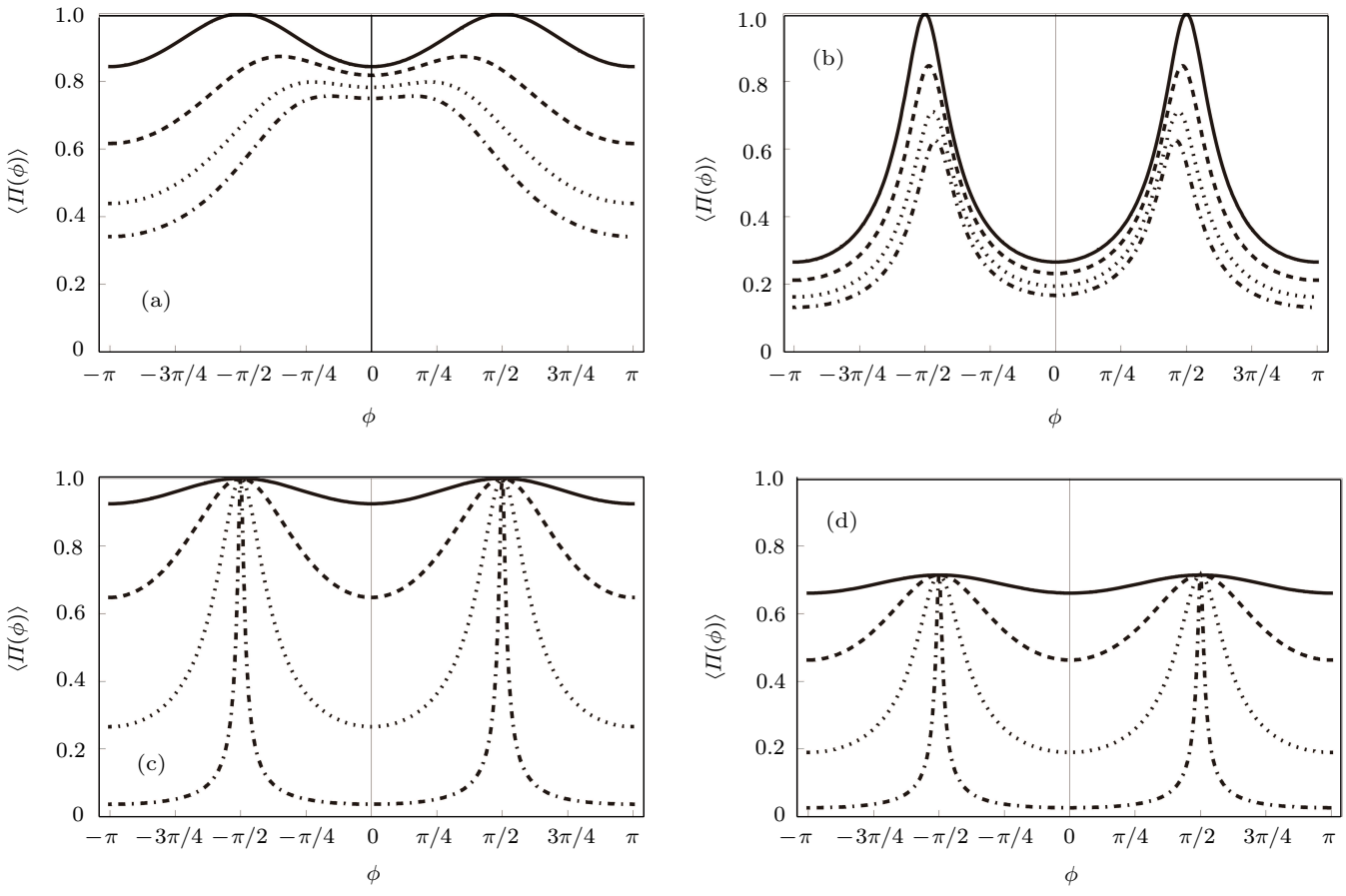


Fig. 2. The parity signal as a function of the shift phase with different input TMSTS. (a) $r = 0.3$, $\bar{n}_1 = 0$ (solid), 0.2 (dashed), 0.5 (dotted), 0.8 (dot–dashed), $\bar{n}_2 = 0$; (b) $r = 1$, $\bar{n}_1 = 0$ (solid), 0.2 (dashed), 0.5 (dotted), 0.8 (dot–dashed), $\bar{n}_2 = 0$; (c) $r = 0.2$ (solid), 0.5 (dashed), 1 (dotted), 2 (dot–dashed), $\bar{n}_1 = 0$, $\bar{n}_2 = 0$; (d) $r = 0.2$ (solid), 0.5 (dashed), 1 (dotted), 2 (dot–dashed), $\bar{n}_1 = 0.2$, $\bar{n}_2 = 0.2$.

In Fig. 2 we plot the parity signal $\langle \Pi_{a_f} \rangle$ as a function of the shift phase ϕ with different input TMSTS according to Eq. (26). The signal of the parity detection scheme is periodic with period 2π. For the symmetrical TMSTS, it is shown from Figs. 2(c) and 2(d) that two peaks of the signal are always found at $\phi = \pm\pi/2$ and the width of each peak becomes narrower with the increasing r. When $\bar{n}_1 = \bar{n}_2 = 0$, it attains its maximum value of one at $\phi = \pm\pi/2$, while this maximum value decreases with the increasing $\bar{n}_1 = \bar{n}_2$, which is independent of the squeezing parameter r. Moreover, for the case of asymmetrical TMSTS with $\bar{n}_1 \neq 0$ and $\bar{n}_2 = 0$ (see Figs. 2(a) and 2(b)), the corresponding maximum value not only becomes smaller but also drifts away from $\phi = \pm\pi/2$ as $\bar{n}_1$ increases. The case of $\bar{n}_1 = 0$ and $\bar{n}_2 \neq 0$ is the same as that of $\bar{n}_1 \neq 0$ and $\bar{n}_2 = 0$.

5. Phase sensitivity

The phase sensitivity is quantified by an average value of how much the measured phase could differ from the actual value. It is an important aspect of optical interferometry. Based on the outcome of the parity measurement ($O = \Pi_{a_f}$), knowing the signal suffices for the sensitivity calculation since $\Pi_{a_f}^2 = 1$, the variance of the phase estimation could be estimated as the following formula

$$\delta\phi^2 = \frac{1 - \langle \Pi_{a_f} \rangle^2}{\left(\partial_\phi \langle \Pi_{a_f} \rangle\right)^2}, \tag{28}$$

which is a ratio of detection noise to the rate at which the signal changes as a function of phase. Therefore, the phase sensitivity in our scheme can be estimated as

$$\delta\phi^2 = H^{-2}\left[\left(J_1\cos^2\frac{\phi}{2} + J_2\sin^2\frac{\phi}{2}\right)^2 - J_3^2\sin^2\phi\right]^2\left[\left(J_1\cos^2\frac{\phi}{2} + J_2\sin^2\frac{\phi}{2}\right)^2 - J_3^2\sin^2\phi - 4H^2\right]$$
$$\times\left[\frac{\left(J_2^2 - J_1^2\right)\sin\phi}{2} - \frac{\left((J_2 - J_1)^2 + 4J_3^2\right)\sin 2\phi}{4}\right]^{-2}. \tag{29}$$

In particular, when $\bar{n}_1 = \bar{n}_2 = \bar{n}$, i.e., the symmetrical TMSTS, leading to $J_2 = J_1 = J$, we have

$$\delta\phi^2|_{\bar{n}_1=\bar{n}_2=\bar{n}} = H^{-2}\left(J_3^2\sin 2\phi\right)^{-2}\left(J^2 - J_3^2\sin^2\phi\right)^2\left(J^2 - J_3^2\sin^2\phi - 4H^2\right). \tag{30}$$

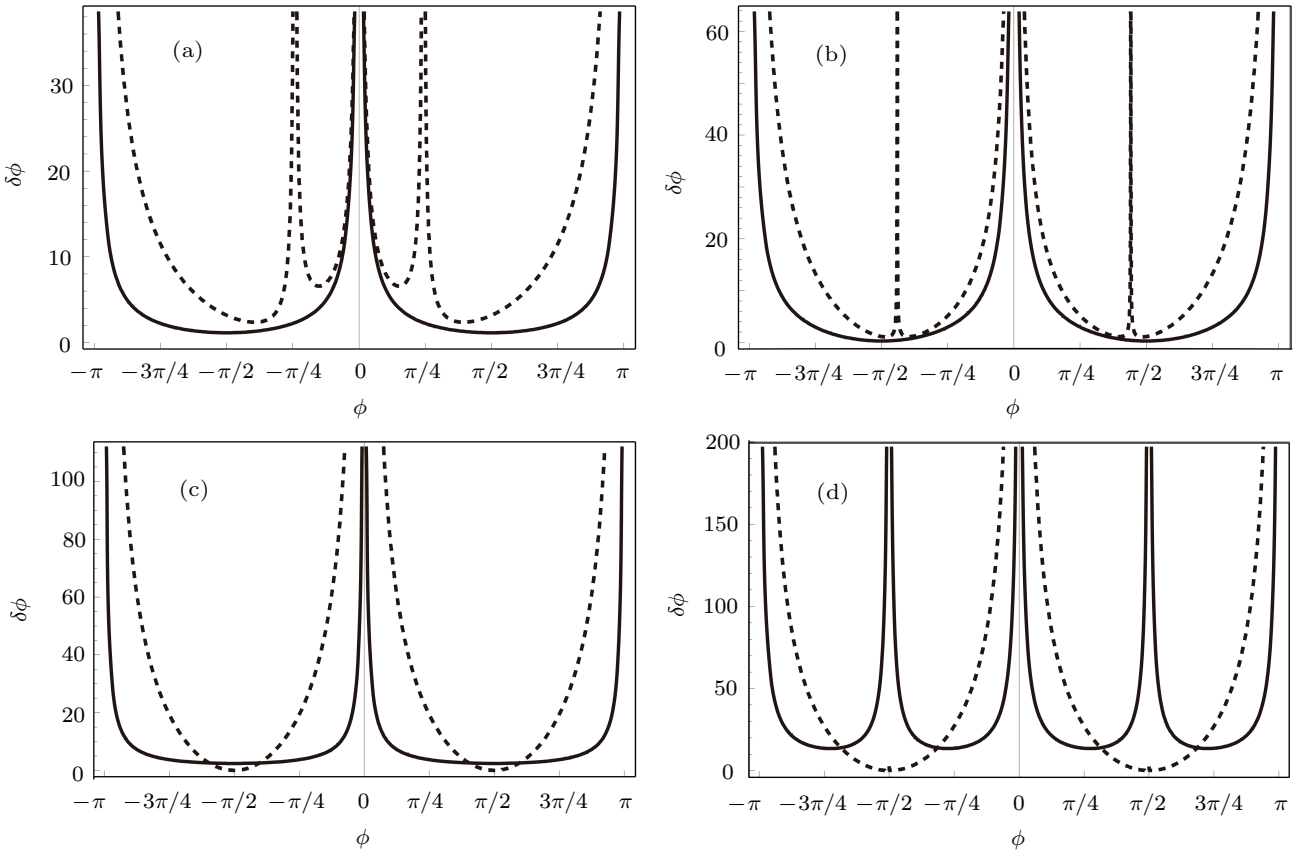


Fig. 3. Phase sensitivity $\delta\phi$ with parity detection as a function of the shift phase ϕ with different input TMSTS. (a) $r = 0.4$, $\bar{n}_1 = 0$ (solid), 2 (dashed), $\bar{n}_2 = 0$; (b) $r = 1$, $\bar{n}_1 = 0$ (solid), 2 (dashed), $\bar{n}_2 = 0$; (c) $r = 0.2$ solid), 2 (dashed), $\bar{n}_1 = 0$, $\bar{n}_2 = 0$; (d) $r = 0.2$ (solid), 2 (dashed), $\bar{n}_1 = 0.2$, $\bar{n}_2 = 0.2$.

To see clearly the behaviors of the phase sensitivity for the different TMSTS, in Fig. 3 we plot phase sensitivity $\delta\phi$ with parity detection as a function of the shift phase ϕ with different input TMSTS according to Eq. (29). In principle, the smaller the value of $\delta\phi$, the higher the phase sensitivity. A numerical calculation of the phase sensitivity for the symmetrical case shows the highest phase sensitivity $\delta\phi$ at the optimal working point being close to $\pi/2$. In addition, the minimum value for $\delta\phi$ is 0.000331577 at the point of $r \to 4.07803$, $\bar{n} \to 0.00270621$, and $\phi \to \pi/2$. In addition, for the asymmetrical case, the optimal working point deviates from $\pi/2$, as shown in Figs. 3(a) and 3(b).

By numerical simulation, we find that one minimum of phase sensitivity is 0.00582434 with $r \to 4.39585$, $\bar{n}_1 \to 2.20112$, $\bar{n}_2 \to 5.39877$, $\phi \to \pi/2$. In the vicinity of this parameter interval, we plot the phase sensitivity $\delta\phi$ as a function of the total photon number $\bar{N}$ by fixing $\bar{n}_1 \to 2.20112$, $\bar{n}_2 \to 5.39877$, $\phi \to \pi/2$, and modulating r between 3.8 and 4.8 (black solid line), SNL (blue dashed line), and HL (red dot–dashed line) in Fig. 4. The curve of phase sensitivity is interchanged with the SNL curve at the threshold value with $\bar{N} = 4 \times 10^4$ and is always above the HL line. The figure demonstrates that $\delta\phi > \delta\phi_{\rm SNL} > \delta\phi_{\rm HL}$ in the interval of $\bar{N} \leq 4 \times 10^4$ and $\delta\phi_{\rm SNL} > \delta\phi > \delta\phi_{\rm HL}$ in the interval of $\bar{N} \geq 4 \times 10^4$. The result shows that only the TMSTS with a large number of photons can beat supersensitivity.

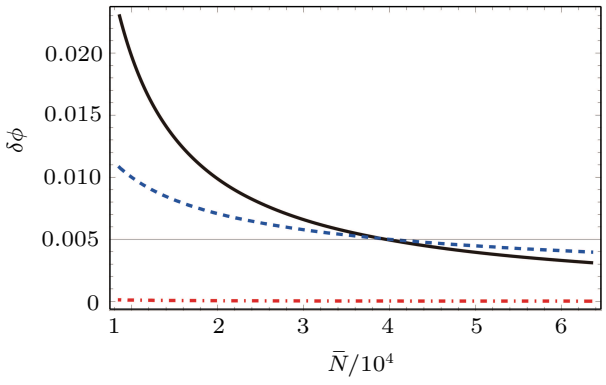


Fig. 4. (color online) Phase sensitivity $\delta\phi$ as a function of the total photon number $\bar{N}$ by fixing $\bar{n}_1 \to 2.20112$, $\bar{n}_2 \to 5.39877$, $\phi \to \pi/2$, and modulating r between 3.8 and 4.8 (black solid line), SNL (blue dashed line), and HL (red dot–dashed line).

To verify our result, we also reduce our work to a similar work with the condition $\bar{n}_1 = \bar{n}_2 = 0$ studied in Ref. [16]. Thus equation (27) is simplified as

$$\left\langle \Pi_{a_f} \right\rangle \Big|_{n_1=n_2=0} = \frac{1}{\sqrt{\cosh^2 2r - \sin^2\phi \sinh^2 2r}} = \frac{1}{\sqrt{1+(\bar{N}^2+2\bar{N})\cos^2\phi}}, \tag{31}$$

where we use the relation $\sinh^2 r = \bar{N}/2$ for TMSVS. Comparing Eq. (31) with Eq. (3) in Ref. [16], the result is consistent, in addition to an additional $\pi/2$ phase shift. If we set $\varphi = \phi - \pi/2$, then we have

$$\langle \Pi_{a_f} \rangle |_{n_1=n_2=0} = 1/\sqrt{1+(\bar{N}^2+2\bar{N})\sin^2\varphi},$$

this expression is identical to just Eq. (3) in Ref. [16]. Subsequently, equation (31) is reduced to

$$\delta\phi|_{n_1=n_2=0} = \frac{1+\bar{N}(\bar{N}+2)\sin^2\varphi}{|\cos\varphi|\sqrt{\bar{N}(\bar{N}+2)}}. \tag{32}$$

It is found that the expression in Eq. (32) is also identical to the result in Ref. [16].

In Fig. 3(c), we can clearly see that phase sensitivity obtained by the parity measurement at $\phi = \pi/2$ saturates the lower bound. Thus by the parity measurement at $\varphi = 0$, the phase sensitivity is

$$\delta\phi|_{n_1=n_2=0} = 1/\sqrt{\bar{N}(\bar{N}+2)},$$

which is shaped in Fig. 5. There is a vicinity around $\varphi = 0$ where phase sensitivity saturates the lower bound defined by the HL.

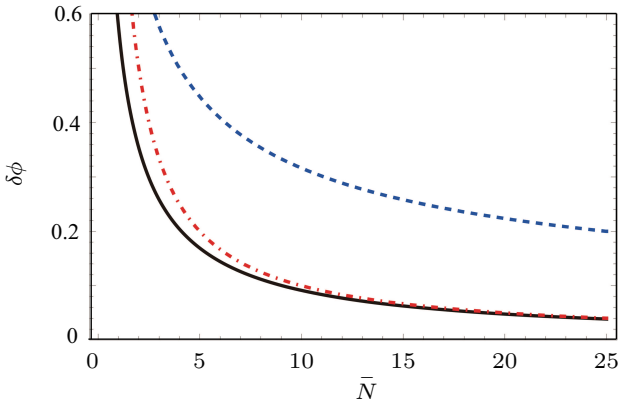


Fig. 5. (color online) Phase sensitivity $\delta\phi$ as a function of the total photon number $\bar{N}$ at $\varphi = 0$ for input TMSVS (black solid line), SNL (blue dashed line), and HL (red dotdashed line).

6. Conclusions

In summary, we have studied the application of parity detection for phase estimation in Mach–Zehner interferometry with a two-mode squeezed thermal state based on the Wigner-function method rather than the traditional operator method. The detected parity is easily obtained from the output WF. The results from the numerical calculation show that the supersensitivity can be reached only if the input TMSTS have a large number photons. Our result can be reduced to the case of the two-mode squeezed vacuum state (TMSVS) in Ref. [16]. On the other hand, the present paper further demonstrates the power of the Wigner-function method in studying quantum optics and quantum metrology.

References

[1] Hariharan P 2003 *Optical Interferometry* (Amsterdam: Elsevier)

[2] Helstrom C W 1976 *Quantum Detection and Estimation Theory, Mathematics in Science and Engineering* (New York: Elsevier Science)
[3] Escher B M, de Matos Filho R L and Davidovich L 2011 *Nat. Phys.* **7** 406
[4] Giovannetti V, Lloyd S and Maccone L 2011 *Nat. Photon.* **5** 222
[5] Yurke B, McCall S L and Klauder J R 1986 *Phys. Rev. A* **33** 4033
[6] Boixo S, Datta A, Davis M J, Flammia S T, Shaji A and Caves C M 2008 *Phys. Rev. Lett.* **101** 040403
[7] Holland M J and Burnett K 1993 *Phys. Rev. Lett.* **71** 1355
[8] Caves C M 1981 *Phys. Rev. D* **23** 1693
[9] Pezzé L and Smerzi A 2008 *Phys. Rev. Lett.* **100** 073601
[10] Seshadreesan K P, Anisimov P M, Lee H and Dowling J P 2011 *New J. Phys.* **13** 083026
[11] Boto A N, Kok P, Abrams D S, et al. 2000 *Phys. Rev. Lett.* **85** 2733
[12] Dowling J P 2008 *Contemp. Phys.* **49** 125
[13] Hu L Y, Wei C P, Huang J H and Liu C J 2014 *Opt. Commun.* **323** 68
[14] Lee S Y, Lee C W, Nha H and Kaszlikowski D 2015 *J. Opt. Soc. Am. B* **32** 1186
[15] Giovannetti V, Lloyd S and Maccone L 2006 *Phys. Rev. Lett.* **96** 010401
[16] Anisimov P M, Raterman G M, Chiruvelli A, Plick W N, Huver S D, Lee H and Dowling J P 2010 *Phys. Rev. Lett.* **104** 103602
[17] Zhang Y M, Li X W and Jin G R 2013 *Chin. Phys. B* **22** 114206
[18] Ekert A K and Knight P L 1991 *Phys. Rev. A* **43** 3934
[19] Suda M 2006 *Quantum Interferometry in Phase Space* (Berlin/Heidelberg: Springer-Verlag)
[20] Schleich W P 2001 *Quantum Optics in Phase Space* (Berlin: Verlag)
[21] Xu X X, Jia F, Hu L Y, Duan Z L, Guo Q and Ma S J 2012 *J. Mod. Opt.* **59** 1624
[22] Xu X X and Yuan H C 2015 *Quantum Inform. Process.* **14** 411
[23] Hu L Y, Wang S and Zhang Z M 2012 *Chin. Phys. B* **21** 064207
[24] Hu L Y, Fan H Y and Zhang Z M 2013 *Chin. Phys. B* **22** 034202
[25] Fan H Y, Lu H L and Fan Y 2006 *Ann. Phys.* **321** 480
[26] Fan H Y, Lu H L, Gao W B and Xu X F 2006 *Ann. Phys.* **321** 2116
[27] Meng X G, Wang J S and Liang B L 2009 *Chin. Phys. B* **18** 1534
[28] Meng X G, Wang Z, Fan H Y, Wang J S and Yang Z S 2012 *J. Opt. Soc. Am. B* **29** 1844
[29] Campos R A, Gerry C C and Benmoussa A 2003 *Phys. Rev. A* **68** 023810